Preprints of the 18th IFAC World Congress
Milano (Italy) August 28 - September 2, 2011

Low Speed Control of an Autonomous Vehicle by Using a Fractional PI Controller ⋆

Inés Tejado * **Vicente Milanés** ** **Jorge Villagrá** **
Jorge Godoy ** **Hassan HosseinNia** * **and Blas M. Vinagre** *

* *Industrial Engineering School, University of Extremadura
06006 Badajoz, Spain
(e-mails: {itejbal,hoseinnia,bvinagre}@unex.es)*
** *AUTOPIA Program, Center for Automation and Robotics
(CAR, UPM-CSIC)
28500 Arganda del Rey, Madrid, Spain
(e-mails: {vicente.milanes,jorge.villagra,jorge.godoy}@csic.es)*

Abstract: Highly non-linear vehicle dynamics plays an important role in autonomous driving systems, especially in congested traffic situations at very low speeds. Due to this fact, accurate controllers are needed in order to ensure safety during navigation. This paper focuses on the design and experimental implementation of a fractional PI$^\alpha$ controller for the low speed control problem in an autonomous prototype Citroën vehicle. Experimental tests at low speeds, obtained with a real vehicle on a real circuit at the Center for Automation and Robotics facilities, show the effectiveness of the proposed controller.

Keywords: Road Vehicle Control, Linear Model, Longitudinal Control, PI$^\alpha$.

1. INTRODUCTION

Nowadays, the idea of automatic vehicles driving in an automatic way is a far aim. Some advances oriented to this target have been achieved notwithstanding. Tasks, such as parking assistance or keeping a safe distance from other vehicles, have been implemented in commercial vehicles during the last years. Most of these advances focus on improving the passengers and pedestrians safety in the surrounding area. However, human failures keep being the main cause of serious accidents.

Up to now, advanced driver assistance systems (ADAS) have been developed to aid drivers in highways as adaptive cruise control (ACC) systems (see Naranjo et al. (2007)). However, urban environments deserve more attention since traffic accidents mainly occur in populated areas. From the ADAS development point of view, the main problem is due to the fact vehicle's behaviors in urban environments are unpredictable.

Automotive sector has included in its commercial vehicles some advances for driving in urban areas. From the efficiency point of view, the Start&Stop system in Plá (2009) permits switching off the vehicle's engine when it is stopped because of traffic lights or jams. So, CO_2 emissions are significantly reduced. Nevertheless, from the safety point of view, autonomous systems capable of aiding the driver in case of congested traffic situations still remain as an unsolved problem. The main difficulty arises from the highly non-linear dynamics of vehicles at very low speeds.

⋆ This work has been supported by the Spanish MICINN research projects TRA2008-06602-C03-01 and TRA2008-06602-C03-02.

Fractional order control (FOC), that is, the generalization to non-integer orders of traditional controllers or control schemes, and its applications are becoming an important issue since it translates into more tuning parameters or, in other words, more adjustable time and frequency responses of the control system, allowing the fulfilment of robust performances. It has been applied, in a satisfactory way, in several automatic control applications (see Monje et al. (2010), Chen et al. (2009) and references therein) leading to the conclusion that FOC is preferred to other techniques (the better performance of this type of controllers, in comparison with the classical PID ones, has been demonstrated e.g. in Oustaloup (1991) and Podlubny (1999)). However, FOC has not been applied to low speed control of autonomous vehicles, expecting robust results.

With the above motivation, this paper deals with the design and implementation –using an experimental vehicle in a real environment– of a fractional PI$^\alpha$ controller to perform the vehicle longitudinal control autonomously at low speeds. The present communication is part of a collaboration between the AUTOPIA program of the Center for Automation and Robotics (CAR, CSIC-UPM) and the University of Extremadura. Its aim is to develop a system capable of performing longitudinal control of a commercial vehicle using as input data on-board vehicle sensors and a fractional controller to manage vehicle's actuators autonomously.

The remaining of this paper is organized as follows. Section 2 includes the description of the experimental vehicle tested in this work, as well as its identified linear model. The design process of the fractional controller and some

details of its implementation are included in Section 3. Section 4 presents the obtained experimental results. The concluding remarks and future work are outlined in Section 5.

2. EXPERIMENTAL VEHICLE

The goal of this work is not only designing a fractional PI$^{\alpha}$ controller for the longitudinal control of an autonomous vehicle but also implementing this system in a prototype vehicle with automatic driving capabilities so as to check its behavior in an environment as real as possible. In this section, the description of the experimental vehicle –a commercial convertible Citroën C3 Pluriel described in Milanés et al. (2010b) (see Fig. 1)– and its modifications to autonomously act over the throttle and brake pedals –i.e. longitudinal control– are provided. A linearized dynamic longitudinal model at low speeds is also included, obtained from experimental results.

Fig. 1. Experimental vehicle at the Center for Automation and Robotics

2.1 Description of the prototype

The experimental vehicle's throttle is controlled with an analog signal that represents the pressure on the pedal, generated with an analog card. A switch has been installed in the dashboard to change from the automatic throttle control to the original throttle circuit.

For the brake's automation, it is imposed as prerequisite to obtain a brake-by-wire system capable of working in parallel with the original braking circuit. To this aim, two shuttle valves are connected to the input of the anti-lock braking system (ABS) in order to keep the two circuits independent. The autonomous action over the brake is governed by an electrohydraulic braking system. A CAN digital-analog input-output device is in charge of managing the control valves (refer to Milanés et al. (2010a) for more details).

Concerning the control algorithm, an on-board control unit (OCU) has been installed in the trunk. The control algorithm is running in real time in the OCU and the generated control actions are sent to the control devices which govern the actuators.

With respect to the sensorial information, a real time kinematic-differential global positioning system (RTK-DGPS), combined with an inertial measurement, are used for vehicle's positioning, proposed in Milanés et al. (2008). Furthermore, the information coming from the on-board sensors –speed, acceleration, current gear, etc.– are acquired via controller area network (CAN) bus.

2.2 Dynamic longitudinal model

Due to the impossibility of obtaining the exact dynamics that describes the vehicle, in this work the idea is to obtain a simple linear model of the vehicle for the circuit wherein the experimental manœuvres will be performed.

To do so, a chirp signal is used as the input signal of the vehicle throttle, as shown in Fig. 2 –solid blue line–, where the dashed red line corresponds to the slope angle of the circuit. In this case, the experimental vehicle response is plotted in Fig. 3 –solid blue line–, which includes the vehicle inherent dynamics and the environment and circuit perturbations, such as the slope of the circuit. Including the vehicle interaction with the terrain during the identification of vehicle dynamics is commonly used in the vehicles literature (see e.g. Rodríguez Castaño (2007) and references therein). The identification process is carried out by means of the *Identification Toolbox* of Matlab based on the frequency domain, considering the mentioned input and the experimental response and selecting a second order model for the approximation. However, the vehicle longitudinal dynamics can be even simplified by the following first order transfer function:

$$G(s) \simeq \frac{K}{s+p} = \frac{4.39}{s+0.1746}, \tag{1}$$

which corresponds with the dashed red line in Fig. 3. Simple linear longitudinal models has been also used in Rodríguez Castaño (2007) and Kamga and Rachid (1996). The reason why there is no need to use a more complex model arises from the kind of manœuvres we perform in this work, as will be stated from the experimental results.

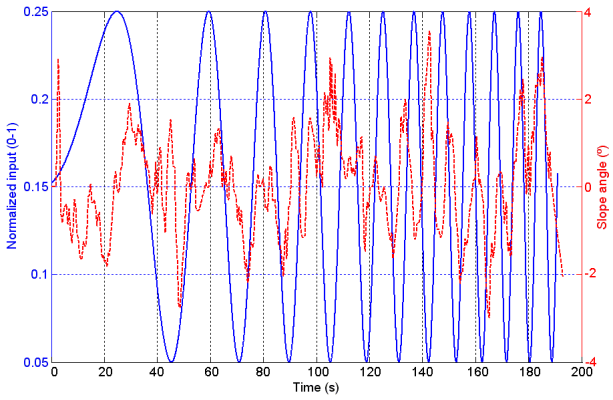

Fig. 2. Normalized input –in the interval $(0, 1)$– to the throttle and the circuit slope

It is important to remark that the identification process is carried out only acting over the throttle. The identification of the vehicle dynamics during braking is neglected because of two reasons: 1) since target speeds are set lower than 15km/h, the vehicle always remains in first gear (with a high engine braking force); 2) the automated braking system (see Milanés et al. (2010a)) has been designed for emergency braking situations at high speeds so a minimum action over the brake at lower speeds causes a significant deceleration. Bearing this in mind and, for simplicity, the action over the brake is limited for this application.

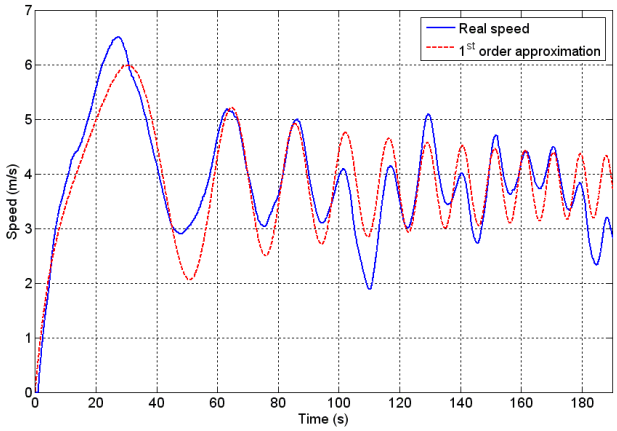

Fig. 3. Experimental vehicle response for the identification of its longitudinal dynamics

3. CONTROLLER DESIGN

For low speed control purposes, the most important mechanical and practical requirements of the vehicle to take into account during the design process are the following:

- The control action has to belong to the interval $(-1, 1)$, where the negatives values means a brake action and the positives, a throttle action.
- The vehicle response has to be smooth to guarantee that its acceleration will be less than the well-known comfort acceleration, that is, less than 2m/s^2.

Apart from the inherent vehicle issues, the controller will have a twofold purpose: 1) robustness against non-modeled dynamics and imprecision in measurements; and 2) the desired closed loop response has to have a value of overshoot Mp close to 0% and a rise time $t_r \simeq 4$s, or equivalently, a phase margin and a crossover frequency around 90deg and 0.45rad/s, respectively (it has been tested that higher values of both parameters cause worse system performances –see Onieva et al. (2010) and Villagrá et al. (2010) and the references therein).

In previous works, some traditional PI controllers have been designed with non-significantly good results (refer e.g. to Villagrá et al. (2010)). Due to this fact, and taking into account that fractional order controllers have been applied in several fields with better results in comparison with the traditional ones (see Podlubny (1999)), a PI$^\alpha$ controller, given by (2), is designed to fulfill the desired system specifications. It is important to remark that the use of a PID controller instead of the proposed PI$^\alpha$ might introduce problems with high frequency noise since the derivative action is sensitive to measurement noise.

$$C(s) = k_p + \frac{k_i}{s^\alpha} = k_p\left(1 + \frac{z_c}{s^\alpha}\right), \text{ with } z_c = k_i/k_p. \quad (2)$$

Let assume that the gain crossover frequency is given by ω_c, the phase margin is specified by φ_m and the output disturbance rejection is defined by a desired value of a sensitivity function $S(s)$ for a desired frequencies range. For meeting the system stability and robustness, the three specifications to fulfill are the following:

1. Phase margin specification:

$$Arg[G_{ol}(j\omega_c)] = Arg[C(j\omega_c)G(j\omega_c)] = -\pi + \varphi_m. \quad (3)$$

2. Gain crossover frequency specification:

$$|G_{ol}(j\omega_c)| = |C(j\omega_c)G(j\omega_c)| = 1. \quad (4)$$

3. Output disturbance rejection for $\omega \leq \omega_s = 0.035$rad/s:

$$|S(j\omega)|_{dB} = \left|\frac{1}{1 + C(j\omega)G(j\omega)}\right|_{dB} \leq -20dB, \ \omega \leq \omega_s. \quad (5)$$

The frequency response function of (1) can be expressed as:

$$G(j\omega) = K\left(\frac{p}{\omega^2 + p^2} - j\frac{\omega}{\omega^2 + p^2}\right). \quad (6)$$

So its phase and gain are given by expressions (7) and (8), respectively.

$$Arg\left[G(j\omega)\right] = -\arctan\left(\frac{\omega}{p}\right), \quad (7)$$

$$|G(j\omega)| = K\frac{\sqrt{\omega^2 + p^2}}{\omega^2 + p^2} = \frac{K}{\sqrt{\omega^2 + p^2}}. \quad (8)$$

In accordance with the PI$^\alpha$ controller transfer function form (2), its frequency response function can be expressed as follows:

$$C(j\omega) = k_p\left(1 + \frac{z_c}{j\omega^\alpha}\right) = \\ = k_p\left[1 + z_c\omega^{-\alpha}\cos\phi - jz_c\omega^{-\alpha}\sin\phi\right], \quad (9)$$

being $\phi = \frac{\alpha\pi}{2}$. Thus, its phase and gain are given by expressions (10) and (11), respectively.

$$Arg\left[C(j\omega)\right] = -\arctan\left[\frac{z_c\omega^{-\alpha}\sin\phi}{1 + z_c\omega^{-\alpha}\cos\phi}\right], \quad (10)$$

$$|C(j\omega)| = k_p\sqrt{(1 + z_c\omega^{-\alpha}\cos\phi)^2 + (z_c\omega^{-\alpha}\sin\phi)^2}. \quad (11)$$

Therefore, the phase and gain of the open loop frequency response $G_{ol}(j\omega)$ can be written as:

$$Arg\left[G_{ol}(j\omega)\right] = Arg\left[C(j\omega)\right] + Arg\left[G(j\omega)\right] = \\ = -\arctan\left[\frac{z_c\omega^{-\alpha}\sin\phi}{1 + z_c\omega^{-\alpha}\cos\phi}\right] - \arctan\left(\frac{\omega}{p}\right), \quad (12)$$

$$|G_{ol}(j\omega)| = |C(j\omega)|\,|G(j\omega)| = \\ = \frac{Kk_p\sqrt{(1 + z_c\omega^{-\alpha}\cos\phi)^2 + (z_c\omega^{-\alpha}\sin\phi)^2}}{\sqrt{\omega^2 + p^2}}. \quad (13)$$

Specification 1 leads to

$$-\arctan\left[\frac{z_c\omega_c^{-\alpha}\sin\phi}{1+z_c\omega_c^{-\alpha}\cos\phi}\right]-\arctan\left(\frac{\omega_c}{p}\right)=-\pi+\varphi_m. \tag{14}$$

Then, the relationship between z_c and α can be established as:

$$z_c=\frac{-\tan\left[\arctan\left(\frac{\omega_c}{p}\right)+\varphi_m\right]}{\omega_c^{-\alpha}\left\{\sin\phi+\cos\phi\tan\left[\arctan\left(\frac{\omega_c}{p}\right)+\varphi_m\right]\right\}}. \tag{15}$$

In agreement with specification 2,

$$\frac{Kk_p\sqrt{\left(1+z_c\omega_c^{-\alpha}\cos\phi\right)^2+\left(z_c\omega_c^{-\alpha}\sin\phi\right)^2}}{\sqrt{\omega_c^2+p^2}}=1$$

$$K^2k_p^2\left[1+z_c^2\omega_c^{-2\alpha}+2z_c\omega_c^{-\alpha}\cos\phi\right]=\omega_c^2+p^2. \tag{16}$$

So, the following expression is obtained:

$$k_p^2+k_i^2\omega_c^{-2\alpha}+2k_pk_i\omega_c^{-\alpha}\cos\phi=\frac{\omega_c^2+p^2}{K^2}. \tag{17}$$

And finally, specification 3 can be written:

$$|S|=\left|\frac{1}{1+k_p\left[1+z_c\omega^{-\alpha}\cos\phi-jz_c\omega^{-\alpha}\sin\phi\right]\left(\frac{K}{j\omega+p}\right)}\right|. \tag{18}$$

Solving the set of equations (15), (17) and (18) with the Matlab function *fsolve*, the values of the controller parameters are: $k_p = 0.09$, $k_i = 0.025$ and $\alpha = 0.8$. Figure 4 shows the Bode plot of the controlled system by applying the designed controller. As it can be observed, the cross over frequency is $\omega_c = 0.46$rad/s and the phase margin is $\varphi_m = 87.79$ deg, fulfilling the design specifications, roughly. Moreover, we force the magnitude of the sensitivity function $S(s)$ to be less than 20dB for frequencies $\omega \leq \omega_s = 0.035$rad/s, which is also fulfilled as illustrated in Fig. 5.

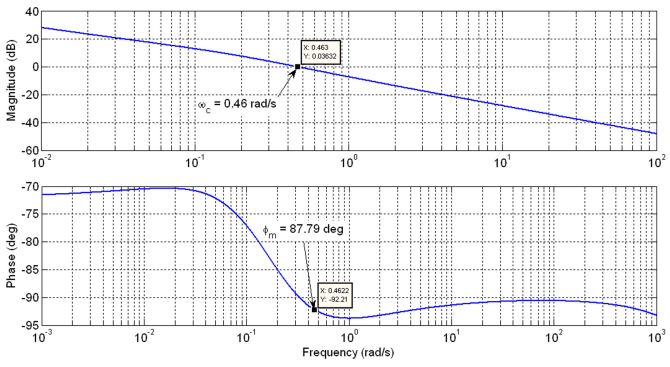

Fig. 4. Bode plot of the controlled vehicle by applying the designed PI$^\alpha$ controller

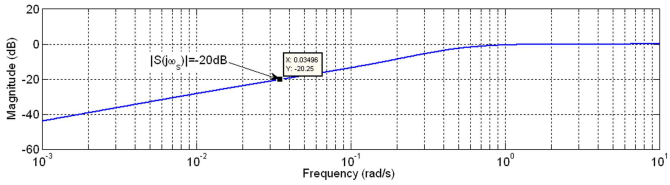

Fig. 5. Magnitude of the sensitivity function $S(s)$

It has to be taken into account that a fractional order controller is an infinite-dimensional linear filter, and that all existing implementation schemes are based on finite-dimensional approximations. In practice, a digital method is used, specifically the indirect discretization method, which requires two steps: firstly, obtaining a finite-dimensional continuous approximation, and, secondly, discretizing the resulting s-transfer function. In our case, in order to preserve the integral effect, the fractional integral $s^{-0.8}$ has been implemented as follows:

$$\frac{1}{s^{0.8}}=\frac{1}{s}s^{0.2}.$$

Therefore, only the fractional part $R_d(s) = s^{0.2}$ will be approximated.

To obtain a finite-dimensional continuous approximation of this fractional order differentiator, the Oustaloup's method is used (see Oustaloup (1991)). An integer order transfer function that fits the frequency response of the fractional order integrator $R_d(s)$ in the range $\omega \in (10^{-3}, 10^3)$rad/s is obtained, with 7 poles and 7 zeros. Later, the discretization of this continuous approximation is carried out by using the Tustin rule with a sampling period $T_s = 0.2$s –GPS sampling period–, obtaining the following 7th-order digital IIR filter:

$$R_d(z)=\frac{\sum_{k=0}^{7}b_kz^{-k}}{1+\sum_{k=1}^{7}a_kz^{-k}}, \tag{19}$$

where $b_0 = 0.1573$, $b_1 = 0.1325$, $b_2 = -0.4389$, $b_3 = -0.3658$, $b_4 = 0.406$, $b_5 = 0.3342$, $b_6 = -0.1244$, $b_7 = -0.1009$, $a_1 = -0.8662$, $a_2 = -2.746$, $a_3 = 2.339$, $a_4 = 2.507$, $a_5 = -2.095$, $a_6 = -0.7602$ and $a_7 = 0.6211$. Therefore, the resulting total fractional order controller is an 8th-order digital IIR filter given by:

$$C(z)=0.09+0.025\left(\frac{1-z^{-1}}{T_s}\right)R_d(z).$$

Figures 6 and 7 show the influence of the fractional order α of the PI$^\alpha$ controller (2) in the time domain by means of the step response –for a desired speed of 8km/h– and the control action and in the frequency domain by means of the Bode plots, where the PI controller is given by $k_p = 0.09$ and $k_i = 0.025$. As it can be stated, the higher the value of α, the higher the overshoot and the lower the control action in Fig. 6. On the other hand, considering the Bode plots in Fig. 7, with a PI$^\alpha$ controller is possible to obtain a controlled system with a similar crossover frequency and phase at high frequencies and different stability margins.

Specifically, the higher the value of α, the higher the phase margin.

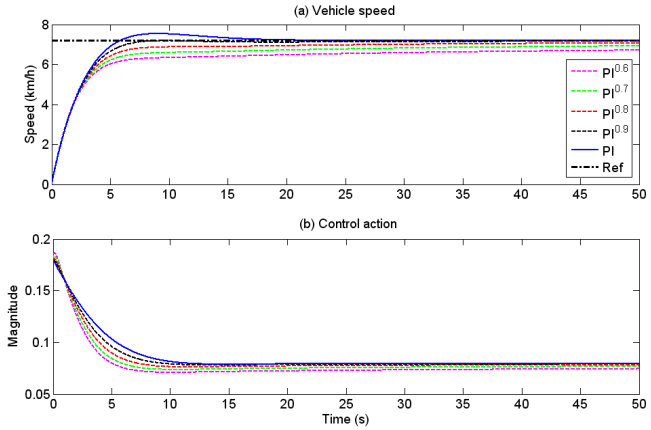

Fig. 6. Step responses by applying a PI$^\alpha$ controller with different values of the order α: (a) Vehicle speed (b) Control action

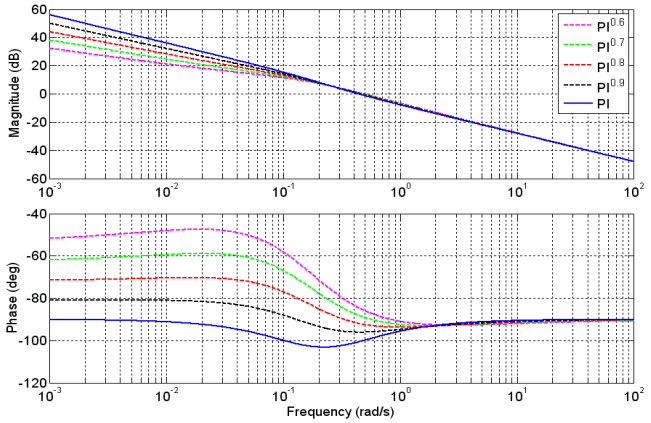

Fig. 7. Bode plots by applying a PI$^\alpha$ controller with different values of the order α

4. EXPERIMENTAL RESULTS

The controller has been tested in simulation and on the real vehicle in the CAR's private driving circuit illustrated in Fig. 8. This circuit has been designed with scientific purposes so only experimental vehicles are driven in this area. It includes 90 deg bends and different slopes so as to validate the controller in different circumstances as close to a real environment as possible.

Fig. 8. Private driving circuit at the Center for Automation and Robotics

Figure 9 shows the real behavior of the autonomous vehicle by applying the designed PI$^\alpha$ controller. In (a), the solid blue line refers to the obtained experimental response, whereas the dashed green one corresponds to the simulated one. In principle, it is worth mentioning that both responses, experimental and simulated, are quite similar, so, as mentioned before, the obtained model for the longitudinal dynamics of the vehicle is good enough for the considered manœuvres at low speeds. Besides, it is important to remark that the vehicle behavior is stable and smooth, and the desired comfort acceleration is also fulfilled (see Fig. 9 (b)), keeping the speed error close to zero (in Fig. 9 (c)). For a better interpretation of speed error results, the mean value of the speed error for each stretch is given in Tab. 1, calculating the mean after the transient state. These values are acceptable values for the speed error at low speeds, but it is also worth mentioning that the slope of the circuit considerably affects the vehicle response since the vehicle always remains in first gear and the engine braking force is high. Figure 9 (d) illustrates the throttle –solid blue line– and brake –dashed red line– action, which are inherently in the interval $(-1, 1)$. One can appreciate the soft action over vehicle's actuators obtaining a good comfort for car's occupants –this is reflected in the acceleration values.

Table 1. Mean speed errors

Speed (km/h)	Time interval (s)	Mean error (km/h)
10	$[5, 24]$	0.2495
15	$[35, 50]$	0.1549
8	$[59, 100]$	0.3808

To sum up, fractional order PI$^\alpha$ controllers can be useful controllers to control autonomous vehicles at really low speeds, specially due to its possibility of obtaining more adjustable time and frequency responses and allowing the fulfilment of more robust performances. The vehicle behavior is significantly good, especially concerning the comfort of vehicle's occupants.

5. CONCLUSIONS AND FUTURE WORKS

In this paper, a PI$^\alpha$ controller has been designed and implemented to perform the longitudinal control of a prototype Citroën vehicle autonomously at low speeds. A simple dynamic longitudinal model has been identified and used for the design process, matching the experimental results consistently. The fractional PI$^\alpha$ controller applied has shown a good vehicle performance for changes in navigation speed, especially on the comfort of vehicle's occupants.

Our future research efforts would be in the networked control of autonomous vehicles and the use of fractional order strategies to compensate network induced effects, as the next step in the collaboration project between the Center for Automation and Robotics and the University of Extremadura.

REFERENCES

Chen, Y.Q., Petras, I. and Xue, D. (2009) Fractional Order Control: A Tutorial. In: *Proceedings of the 2009 American Control Conference (ACC'09)*, 1397-1411.

Kamga, A. and Rachid, A. (1996). Speed, Steering Angle and Path Tracking Controls for a Tricycle Robot. In:

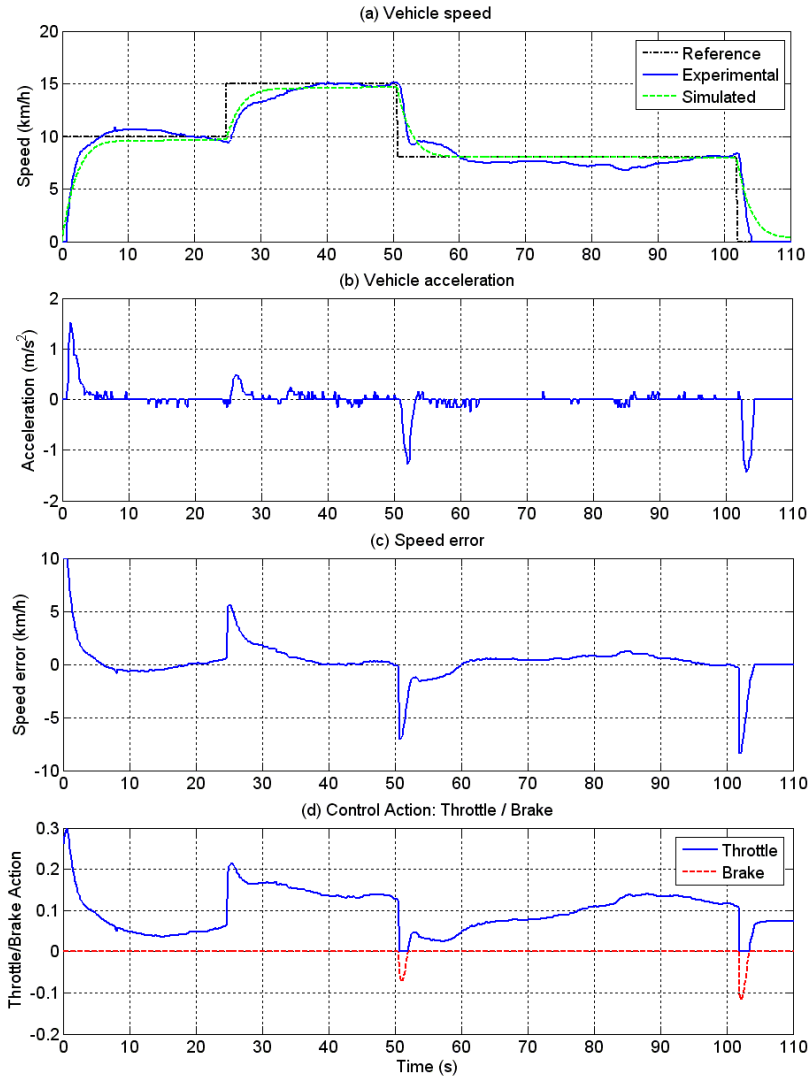

Fig. 9. Vehicle response by applying the PI$^{\alpha}$ controller: (a) Speed –experimental and simulated– (b) Acceleration (c) Speed error (d) Control action

Proceedings of the 1996 IEEE International Symposium on Computer-Aided Control System Design, 56-61.

Milanés, V., González, C., Naranjo, J., Onieva, E., and de Pedro, T. (2010a). Electro-hydraulic Braking System for Autonomous Vehicles. *International Journal of Automotive Technology*, 11(1), 89–95.

Milanés, V., Llorca, D., Vinagre, B., González, C., and Sotelo, M. (2010b). Clavileño: Evolution of an Autonomous Car. In: *Proceedings of the 13th International IEEE Conference on Intelligent Transportation Systems (ITSC'10)*, 1129-1134.

Milanés, V., Naranjo, J.E., González, C., Alonso, J., and de Pedro, T. (2008). Autonomous Vehicle Based in Cooperative GPS and Inertial Systems. *Robotica*, 26(5), 627–633.

Monje, C.A., Chen, Y.Q., Vinagre, B.M., Xue, D., and Feliu, V. (2010). *Fractional-order Systems and Controls. Fundamentals and Applications*. Springer.

Naranjo, J.E., González, C., García, R., and de Pedro, T. (2007). Cooperative Throttle and Brake Fuzzy Control for ACC+Stop\&Go Manœuvres. *IEEE Transactions on Vehicular Technology*, 56(4), 1623–1630. doi:10.1109/TVT.2007.897632.

Onieva, E. and Milanés, V. and González, C. and de Pedro, T. and Pérez, J. and Alonso, J. (2010). Throttle and Brake Pedals Automation for Populated Areas. *Robotica*, 28, 509–516.

Oustaloup, A. (1991). *La Commade CRONE: Commande Robuste d'Ordre Non Entier*. Paris: Hermes.

Plá, J. (2009). An Initiative of the Idea in Favour of Energy Efficiency in Transport. Technical Report, Industry Department.

Podlubny, I. (1999). Fractional-Order Systems and PI$^{\lambda}$D$^{\mu}$ Controllers. *IEEE Transactions on Automatic Control*, 44, 208–214.

Rodríguez Castaño, A. (2007) Estimación de Posición y Control de Vehículos Autónomos a Elevada Velocidad. *PhD Thesis*, University of Sevilla, Spain.

Villagrá, J., Milanés, V., Pérez, J., and de Pedro, T. (2010). Control Basado en PID Inteligentes: Aplicación al Control de Crucero de un Vehículo a Bajas Velocidades. *Revista Iberoamericana de Automática e Informática Industrial*, 7(4), 44–52.